Available online at www.sciencedirect.com

ScienceDirect

Biochimica et Biophysica Acta 1758 (2006) 1797–1808

BIOCHIMICA ET BIOPHYSICA ACTA

BBA

www.elsevier.com/locate/bbamem

In-plane miscibility and mixed bilayer microstructure in mixtures of catanionic glycolipids and zwitterionic phospholipids

C.V. Teixeira [a,*], M. Blanzat [b], J. Koetz [c], I. Rico-Lattes [b], G. Brezesinski [a]

[a] *Max Planck Institute of Colloids and Interfaces, Research Campus Golm, Am Mühlenberg 1, D-14476 Potsdam, Germany*

[b] *Laboratoire IMRCP, UMR CNRS 5623, Université Paul Sabatier, 118 route de Narbonne, F-31062 Toulouse cedex, France*

[c] *Institute of Chemistry, University of Potsdam, Karl-Liebknecht-Str. 24/25, D-14476 Potsdam, Germany*

Received 21 March 2006; received in revised form 29 May 2006; accepted 30 May 2006
Available online 6 June 2006

Abstract

SAXS/WAXS studies were performed in combination with freeze fracture electron microscopy using mixtures of a new Gemini catanionic surfactant (Gem16-12, formed by two sugar groups bound by a hydrocarbon spacer with 12 carbons and two 16-carbon chains) and the zwitterionic phospholipid 1,2-dipalmitoyl-*sn*-glycero-3-phosphocholine (DPPC) to establish the phase diagram. Gem16-12 in water forms bilayers with the same amount of hydration water as DPPC. A frozen interdigitated phase with a low hydration number is observed below room temperature. The kinetics of the formation of this crystalline phase is very slow. Above the chain melting temperature, multilayered vesicles are formed. Mixing with DPPC produces mixed bilayers above the corresponding chain melting temperature. At room temperature, partially lamellar aggregates with local nematic order are observed. Splitting of infinite lamellae into discs is linked to immiscibility in frozen state. The ordering process is always accompanied by dehydration of the system. As a consequence, an unusual order–disorder phase transition upon cooling is observed.

Keywords: SAXS; Bilayer; Gemini surfactant; Ordering process; Anti-HIV; Miscibility

1. Introduction

Compounds which inhibit the HIV infection at the early stages of its replication cycle, such as its adsorption and entry into cells, are candidates for polytherapy with drugs already used in clinics [1,2]. HIV infects human cells through the binding of the viral glycoprotein gp120 to cellular receptors (CD4 and galactosylceramide) [3,4]. One strategy consists in synthesizing analogues of the cellular receptor galactosylceramide to limit HIV infection. Amongst these analogues, a catanionic [5] gemini amphiphile Gem16-12 (Fig. 1) displays both a high anti-HIV activity (IC_{50} = 0.5 μM) with a low cytotoxicity (CC_{50} > 100 μM) [6,7]. The IC 50 (the concentration of compound saving 50% of infected lymphocytes cells) is below the CAC concentration (10 μM) of the Gemini 16-12 showing that the activity is not related to the aggregation state of the compound. In contrast the CC50 (the concentration of compound killing 50% of non-infected lymphocyte cells) is largely over the CAC value. Therefore, the aggregation state of the compound could be responsible for the low toxicity. Thus, we proposed the hypothesis that the compound could form aggregates in which the molecules have all the three chains in a stretched position (as shown in Fig. 1b), leading to a reduced incorporation in membrane cells, at least up to a concentration range of 100 μM and for this reason presenting a low toxicity [8,9]. In order to support this assumption, it is important to verify the possibility of making stable bilayers in a large composition and temperature range and consequently determine the preferential arrangement of Gem16-12 both in pure compound and in phospholipid bilayers.

For glycolipids being bound by ionic non-covalent bonds, in-plane miscibility is not always ensured in the whole phase diagram [10]. In this latter case, the immiscibility is the origin of infinite bilayer to disc transition. However, other transitions have been described in diluted lamellar phases. For a review of disruption of lamellar order associated with dilution of bilayers, see Dubois and Zemb [11].

* Corresponding author. Present address: Universitat Autònoma de Barcelona, Faculty of Medicine, Unity of Biophysics 08193, Cerdanyola del Vallès, Spain. Tel.: +34 935814504; fax: +34 935811907.

E-mail address: CilaineVeronica.Teixeira@uab.es (C.V. Teixeira).

0005-2736/$ - see front matter © 2006 Elsevier B.V. All rights reserved.
doi:10.1016/j.bbamem.2006.05.025

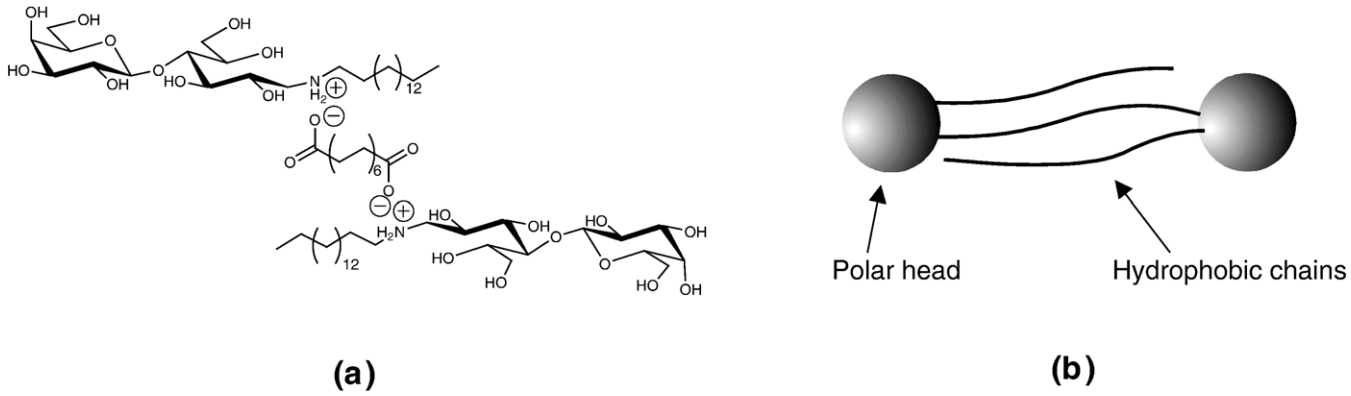

Fig. 1. (a) Chemical structure and (b) schematic representation of gemini catanionic surfactant Gem16-12.

Swelling of mixed lamellar phases including glycolipids also depends on the maximum amount of glycolipids that can be included in a bilayer without in-plane phase separation [12]. Moreover, a complete determination of the ternary phase diagram including a charged synthetic lipid and a glycolipid shows an unusual presence of two critical points at the same osmotic pressure: this means that large changes in composition between two coexisting bilayers respectively rich in the glycolipid component and rich in the lipid component are not associated with large cost in the Gibbs energy [13]. These changes in composition facilitate the curvature and fusion between membranes [14].

Catanionic bilayers can be formed by a chemical acid-base reaction mixing amphiphilic amines with acids as previously described by Blanzat et al. [6,7].

Here we present a SAXS/WAXS combined study above and below the chain melting transition for several molar ratios of the catanionic glycolipid Gem16-12 and the zwitterionic phospholipid DPPC. Association of small angle X-ray scattering (SAXS) at high resolution in a q-range up to 0.3 $Å^{-1}$ and WAXS in the q-range from 1 to 2 $Å^{-1}$ allows the characterization of the thickness of the polar and apolar parts within the conventional description of bilayers as a triple layer with two polar regions embedding an apolar core and the crystallinity state of the hydrophobic, respectively.

2. Experimental section

2.1. Sample preparation

1,2-Dipalmitoyl-*sn*-glycero-3-phosphocholine (DPPC) was purchased from Sigma and used without any further purification. Gemini surfactant was synthesized [7] in Laboratoire IMRCP in Toulouse by reacting in water two initially neutral surfactants, N-hexadecylamino-1-deoxylactitol [15] and 1,12-dodecyldicarboxylic acid. Proton transfer between the carboxylic acid and the amine produces a catanionic pair. Gemini surfactant was weighed and mixed with Millipore™ water and then DPPC powder was added to the solution. The solutions were vortexed and sonicated at 50 °C for homogenization. A total solute concentration of 20 wt.% was used and the molar fraction of Gemini (x=number of moles of Gemini/total number of moles) was varied from 0.085 to 0.334. A sample with 20 wt.% Gemini in water was also prepared. The temperature of the system was first increased from 10 °C to 70 °C by steps of 10 °C, and then decreased from 70 °C to 10 °C to check the reversibility of the structures observed, close to the thermodynamic equilibrium.

2.2. X-ray scattering

Small- and wide-angle X-ray scattering (SAXS and WAXS) experiments were simultaneously performed at the beamline A2, at the storage ring DORIS III of HASYLAB, DESY, in Hamburg. The scattered intensities were measured with linear position-sensitive detectors [16] and the calibration was made with rattail and tripalmitin for SAXS and WAXS, respectively. The measured curves were corrected for the detector response and the background was subtracted after normalization of all the curves with the counting rate of an ionization chamber.

SAXS absolute scale measurements were performed in CEA, Saclay, according to the procedure described by Zemb et al. [17] for the sample Gemini/water and one sample Gemini/DPPC/water and all the SAXS results were re-scaled according to these experiments to be in absolute scale. The normalization was done by choosing a range in the experimental curves after the peak of the form factor, which was free from scattering. Then, the curves were normalized by the area under the curve for the chosen range. A comparison of both data, in absolute scale, is shown in Fig. 2. However, no absolute scale measurement was performed for the WAXS region, which will be presented only in arbitrary units, without any loss of information, as the WAXS regions will be used only to verify the ordering of the hydrocarbon chains.

The form factor in cm^{-1} of a dispersion of locally flat non-homogenous bilayers was calculated according to Cantù et al. [18], modelling the bilayers as a triple film in electron density, suspended in a homogenous buffer:

$$P(q) = \frac{4\pi}{q^2}\sum\left[t_1\left(\rho_{\mathrm{pol}} - \rho_{\mathrm{par}}\right)\frac{\sin(qt_1)}{qt_1} + t_2\left(\rho_{\mathrm{sol}} - \rho_{\mathrm{pol}}\right)\frac{\sin(qt_2)}{qt_2}\right]^2 \quad (1)$$

where $q=(4\pi/\lambda)\sin\theta$ is the scattering vector, Σ is the specific area of the total bilayer (in cm^2/cm^3 of sample), $2t_1$ and $2t_2$ are the hydrophobic core and total thickness, respectively, ρ_{pol}, ρ_{par} and ρ_{sol} are the electron densities of the polar region, paraffinic region and solvent, respectively. The specific area is imposed by the amphiphilic concentration c_s (number of molecules per cm^3) to be $\sum = c_s\sigma$, where σ is the area per molecule at the hydrophobic/hydrophilic interface. In the Gemini/DPPC mixed system, c_s was obtained from the sum of the number of moles of both components in the sample divided by the sample volume, so that the total amount of bilayer per cm^3 of solution was obtained. In this way, the resulting area per molecule represents a value which is averaged for both components. For a flat bilayer:

$$t_1 = V_{\mathrm{par}}/\sigma \text{ and } t_2 = t_1 + \left(V_{\mathrm{pol}} + N_{\mathrm{H}}\cdot V_{\mathrm{w}}\right)/\sigma, \quad (2)$$

being V_{par} and V_{pol} the volumes of the paraffinic and polar parts of the molecule. N_{H} is the number of water molecules bound per headgroup (or hydration number) and V_{w} is the molecular volume of water, equal to 30 $Å^3$. The term "hydration" in the form factor has a very precise meaning in SAXS studies [19]: it includes all water molecules that remain in the headgroup region of the bilayer and are

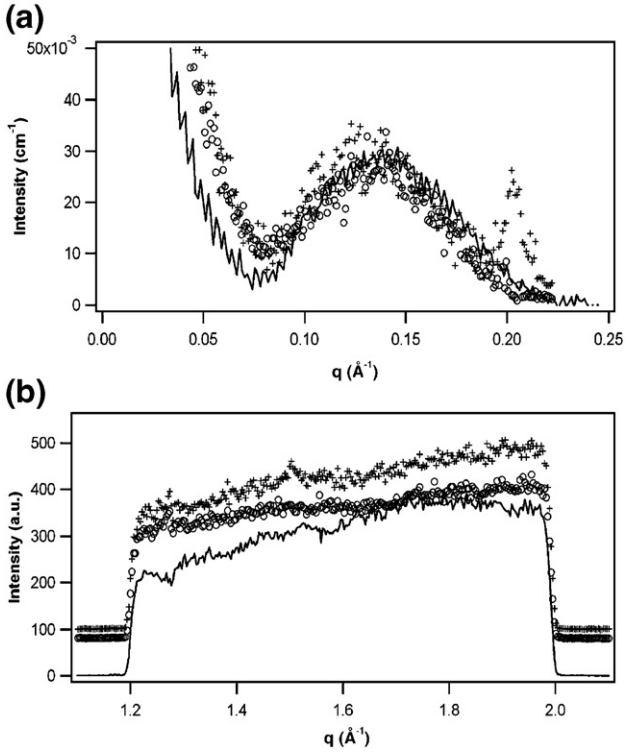

Fig. 2. Scattering curves of the system 20 wt.% Gemini in water at: 20 °C (crosses) and 60 °C (circles). (a) SAXS: solid line shows the data obtained in absolute scale, in CEA, Saclay; (b) WAXS: solid line represents the scattering curve of the water, as reference. WAXS curves are vertically shifted for clarity.

counted in its electron density. The volumes $V_{par(pol)}$, in the case of mixed system, were given by:

$$V_{par(pol)} = V_{par(pol)gemini} \cdot x + V_{par(pol)DPPC} \cdot (1 - x). \quad (3)$$

The electron densities were calculated by:

$$\rho_{pol} = \left(ne_{pol} + ne_{water} \cdot N_H\right)/(t_2 - t_1)\sigma \text{ and } \rho_{par} = ne_{par}/t_1\sigma, \quad (4)$$

where ne_{pol} is the number of electrons in the polar region given by ne_{pol}=number of electrons of Gemini polar head, for the pure Gemini system, and ne_{pol}=(number of electrons of Gemini) x+number of electrons of DPPC·$(1-x)$, for the mixed Gemini/DPPC system. ne_{par} is the number of electrons in the paraffinic region, being : ne_{par}=number of electrons in the hydrocarbon chains (2 tails and spacer) of the Gemini molecule in the case of the pure system and ne_{par}=(number of electrons in the hydrocarbon chains of Gemini) x+(number of electrons in the DPPC hydrocarbon chains)·$(1-x)$. ne_{water} is the number of electrons in a water molecule. ρ_{sol} was 0.33 electrons/Å^3, constant in all fittings.

For the interdependence of the thicknesses and electron densities, t_1 and t_2 were linked by a strong constraint: molecular volume and incompressibility of the sample. Using any fitting procedure in real space as proposed by Glatter et al. does not take into account this strong constraint [20]:

$$t_1 = ne_{par}/\rho_{par}\sigma \text{ and } t_2 = t_1 + \left(ne_{pol} + ne_{water}N_H\right)/\rho_{pol} \cdot \sigma. \quad (5)$$

In this way, from the cross-check of the thickness calculated from the electron density values, we recovered the molecular volume of Gemini.

The broad peak due to the interacting micelles can be described by a nematic phase [21,22], characterized by micelles presenting orientational order but no long-range positional order. Likewise, the broad shoulder present in our scattering curves, at the left side of the peak originated by the form factor, was interpreted as being caused by aggregates with short-range order. This assumption will be proved to be correct by Freeze Fracture Electron Microscopy (FFEM), in the Discussion Section. This system of bilayers lacking long-range order has been largely studied. Structure factors of ordered bilayers with disorder of 1st (thermal disorder, in which the position of each bilayer will oscillate having as reference always the same equilibrium position) and 2nd (where the position of each bilayer is determined by the position of the neighbouring bilayers instead of being determined from an ideal position, so that the deviation from the equilibrium position is increased for each layer) kinds [23] of stacking of bilayers of infinite size in a core-shell-disk model [24], including the effect of finite multilayer domains [25,26] and also including diffuse scattering of single uncorrelated bilayers [27], have been developed. In our case, we stick to the structure factor of stacked bilayers subjected to disorder of second kind [28], especially because our scattering curves are practically dominated by the form factor of the bilayers and the effects of diffuse scattering or decay are hidden. The structure factor is then given by [29]:

$$S(q) = N + 2\sum_{i=1}^{N}(N-i)\cos(qdi)\exp\left(-\frac{i}{2}q^2\Delta^2\right), \quad (6)$$

where N is the number of stacked bilayers, d is the bilayer d-spacing, Δ is the mean square fluctuation of the bilayers, which is higher the more disordered the system is, being $\exp(-q^2\Delta^2/2)$ the Debye–Waller factor.

Thus, for the mixed Gemini/DPPC system, which shows a structure peak besides the form factor of the bilayers, the total scattered intensity is given by:

$$I(q) = (\alpha + S(q))P(q), \quad (7)$$

where α is the number of non-correlated bilayers, which are in the nematic phase.

2.3. Freeze-fracture electron microscopy

Freeze fracture electron microscopy is an excellent method to visualize the individual lamella as well as multilamellar vesicles in lamellar liquid crystalline systems [30]. Samples of 20 wt.% of the product in water were freeze etched starting from 20 °C and 60 °C, respectively, to detect temperature dependent structural changes. Freeze-fracturing, etching and coating were made at either −120 °C or −150 °C using a Balzers BAF 400 freeze-etching unit (Balzers, Liechtenstein). The platinum/carbon coated replicas were cleaned with sulphuric acid. After rinsing in distilled water, the replicas were collected on uncoated copper grids. The cleaned replicas were examined in a transmission electron microscope EM 902 (Zeiss, Germany).

2.4. Differential scanning calorimetry (DSC)

Ultra high resolution DSC-measurements were carried out with a Micro DSC III (Setaram). The samples were cooled down to −20 °C and kept frozen for 5 h. The first heating cycle ends at 80 °C with a second isotherm (15 min). The cooling/heating procedure was repeated several times. Within the experimental precision the different cycles led to the same results. Heating and cooling rates were 0.25 K/min.

3. Results

Pure Gemini surfactant in water solution, as well as mixtures of Gemini surfactant with DPPC at different Gemini molar fractions and different temperatures, were studied. Firstly, we present the scattering curve of pure Gemini in water (Fig. 2) where a broad shoulder centred around q=0.12 Å^{-1} independent of temperature was identified as an oscillation in the form factor.

Fig. 2a exhibits the SAXS curves corresponding to temperatures of 20 °C and 60 °C, illustrating that the non-ordered disk-like aggregates are present at all studied temperatures. However, a sharp peak corresponding to a d-spacing of 31 Å is observed for temperatures of 20 °C and below. This corresponds to a lamellar gel phase with very little water between the bilayers.

Concomitantly, the WAXS curves (Fig. 2b) demonstrate that the hydrocarbon chains are ordered at 20 °C and disordered at 60 °C. The transition was observed at 30 °C. Notice that the peak at 20 °C is not very strong, but can still be detected and shows that the chains are perhaps in a glassy state, less ordered than pure DPPC for instance.

The gemini:DPPC mixtures at low temperatures also present a broad shoulder centred around $q=0.12$ Å^{-1} (Fig. 3), contrarily to what is expected for DPPC in water, indicating that the presence of Gemini destroys the order of the DPPC bilayers. Nevertheless, one should notice a subtle concentration dependent shoulder at lower q-values, evidencing two different contributions to the total scattered intensity: one of these contributions is the form factor of the bilayers (the main broad peak) and the broad shoulder is caused by a structure factor of stacked bilayers lacking long-range order. This effect can be better observed in Fig. 7, which shows the shoulder superposed to the form factor of the bilayer.

The WAXS curves for the mixtures show a peak at low temperatures, but broad compared to the pure DPPC, indicating much smaller positional correlation. At 60 °C, all Gemini/DPPC samples are in the L_α phase, with a sharp peak at (63.5±0.5) Å, and the WAXS curves show that the hydrocarbon chains are molten. However, the transition temperature to the L_α phase depends on the mole fraction of Gemini. A sample with $x=0.167$ forms a well-defined L_α phase already at 50 °C, whereas for $x=0.229$ the formation of this phase is completed only at higher temperatures. At 50 °C, only a small peak at 63.5 Å (circles in the curve) can be seen. This fact shows that the higher the Gemini molar fraction, the higher the transition temperature to a well-defined L_α phase.

4. Discussion

4.1. Binary system of Gemini in water

Gemini surfactant in water exhibits a phase separation below 20 °C. Well-ordered bilayers with a d-spacing of 31 Å coexist with non-ordered, non-correlated bilayers. This corresponds to tie-lines in the phase diagram, as in other charged bilayer systems [31]. The ordered phase was more prominent in samples stored in fridge for a long time. In the samples kept in the fridge at 4 °C for 3 days, the ratio between the intensities of the sharp to the broad peaks was 0.74, whereas for the samples stored at room temperature it was only 0.28. Besides, this phase was not recovered during the measurements when the samples were cooled down after being heated to 70 °C. This means that the nucleation of small crystallites containing ordered bilayers needs a long time and is kinetically hindered. Therefore, the ordered phase coexists with the non-ordered phase, which is kinetically stable bellow and thermodynamically stable above the transition temperature. At high temperatures, only the non-correlated bilayers are present. This statement was confirmed by freeze fracture electron microscopy, where one could see stacked non-fracturable bilayers [8] at a concentration of 20 wt.% of Gemini in water.

The form factor oscillation of the curves was fitted on absolute scale by using Eq. (1), and the results are shown in Table 1. A typical result of a fitting procedure is shown in Fig. 4, together with the form factor calculated by varying the area per molecule (and consequently the layer thickness – t_2) by 10%, in order to illustrate the sensitivity of the method. The hydration number, as well as the area per molecule, remained constant in the whole temperature range studied. The obtained values of t_1 (half the thickness of the hydrocarbon region) and t_2 (half thickness of total

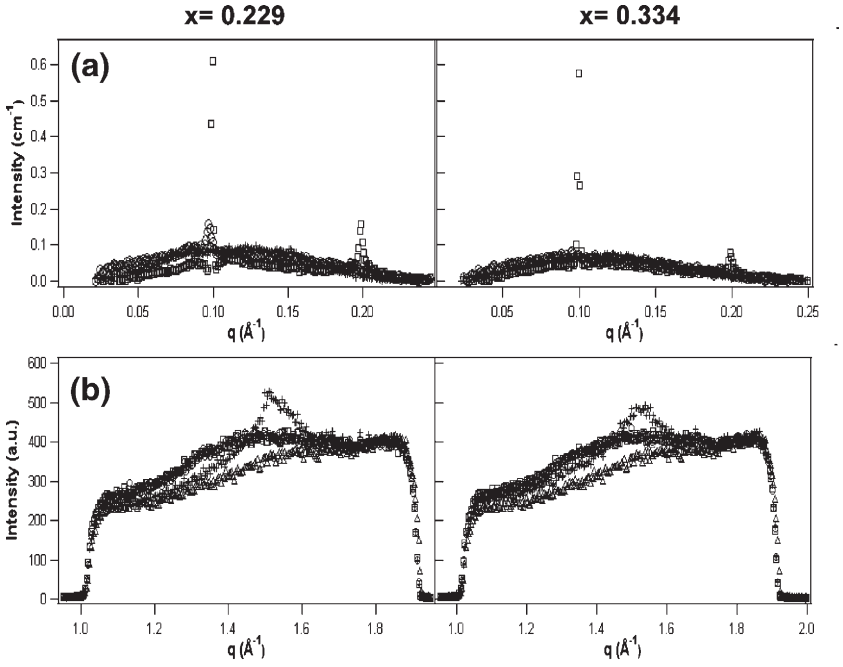

Fig. 3. Scattering curves of the system Gemini/DPPC/water, at approximately 20 wt.% of Gemini + DPPC in water for Gemini molar fractions of 0.229 and 0.334, at: 20 °C (crosses), 50 °C (circles) and 60 °C (squares). (a) SAXS; (b) WAXS: triangles represent the scattering curve of the water, as reference.

Table 1
Parameters obtained from the fitting of form factor of disk-like objects

Parameter	Gemini/water							Gemini/DPPC/water	
Area (Å^2)	58.8 ± 1.5							82	
								50 °C	Other T
N_H	7.3 ± 0.5							9 ± 2	24[(1)]
ρ_{pol} (electrons/Å^3)	0.462							0.400	0.382
ρ_{par} (electrons/Å^3)	0.326							0.279	
	10 °C	20 °C	30 °C	40 °C	50°C	60 °C	70 °C		
t_1 (Å)	19.3	18.6	17.9	18.9	18.3	18.2	18.3	11.5	
								50 °C	Below Tc
t_2 (Å)	37.8	36.4	34.7	35.0	35.2	35.3	35.5	22.2	27[(2)]

[(1)] is an average value of the obtained values for all temperatures below and above the transition temperature.
[(2)] is an average value for all temperatures below the transition temperature.

bilayer) are shown in Fig. 5. Both parameters are nearly constant around an average value of (18.4±0.5) Å for t_1 and (36±1) Å for t_2. This shows that the hydrocarbon chains are disordered at all temperatures investigated and that the overall thickness of the bilayer does not change, indicating a constant hydration value as well. The value of 18 Å obtained for t_1 is very reasonable for disordered C16-chains. The headgroup layer has a length of 18 Å, suggesting an extended conformation of the sugar head group, which is supported by the rather small area per molecule of 59 Å^2, for two sugar groups. From the values obtained for area per molecule, electron density and bilayer thickness, and making use of Eqs. (2) Eqs. (3) Eqs. (4) Eqs. (5), one obtains a molecular density of 1.2 g/cm^3 for Gemini. The values presented in the literature for the density of sugar surfactants vary from 1.06 g/cm^3 [32] (for dodecyl-malono-bis-N-methylglucamide (DBNMG) in SDS micelles studied by Electron Paramagnetic Resonance) to 1.72 g/cm^3, for lactose-based surfactants [33]. Bales et al. [34] found theoretically a molecular density for DBNMG of 1.18 g/cm^3, which is very close to the value obtained by us.

The portion of sample that presents a d-spacing of 31 Å exhibits ordered hydrocarbon chains. The possible configurations of the Gemini molecule within the gel bilayer are presented in Fig. 6. Let us first consider the possibilities for configuration in Fig. 6a: if the C16 chains are in all-trans conformation, they have 20 Å each. Thus, the bilayer would be too thick for the obtained d-spacing of 31 Å. So if we consider that the chains are interdigitated, the back-folded spacer does not allow their complete interdigitation and the bilayer will still be too big for the found d-spacing. Therefore, the conformation of Fig. 6a is not possible for the portion of sample in the ordered phase. Let us then consider the conformation presented in Fig. 6b: the extended C12 chain has approximately 15 Å, shorter than the C16 chains. This means that the longer chains are disordered and/or can be slightly extended towards the hydrophilic region. In this configuration we have 16 Å available to be occupied by the two headgroups (at each end of the bilayer) plus the inter-bilayer water. We know that the sugar headgroups have approximately 18 Å. This means that the headgroups should be strongly tilted and covering the area of three hydrocarbon tails. Such a conformation was suggested by Brun et al. [9] based on monolayer experiments. This phase seems to be poorly hydrated. Stacks of Gemini were also observed by Blanzat et al. in a concentration range of 40–80 wt.% of Gemini in water (little hydration), where the stacks formed spherulites and exhibited no phase transition upon heating [6]. On the other hand, the coexisting nematic phase seems to have much more water between the aggregates, and a number of hydration water molecules of 7.3.

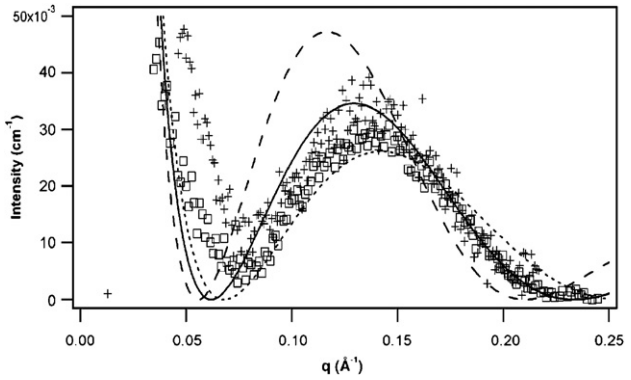

Fig. 4. SAXS curve of 20 wt.% Gemini in water at 40 °C. Crosses: experimental curve (A2 beamline, HASYLAB at Desy); squares: experimental curve measured in CEA, Saclay; solid line: modelled form factor (area per molecule=58.8 Å^2, number of bound water molecules per polar head=7.3, ρ_{pol}=0.462 electrons/Å^3, t_1=18.1 Å, t_2=35 Å); dotted line: calculated form factor with a variation of 10% of area per molecule (higher) (area per molecule=64.6 Å^2, t_1=16.8 Å, t_2=32.5 Å); dashed line: calculated form factor with area per molecule 10% smaller (area per molecule=53.0 Å^2, t_1=20.4 Å, t_2=39.6 Å).

4.2. Ternary system Gemini/DPPC/water

The curves were fitted by using Eq. (7) (through Eqs. (1) and (6)). Fig. 7 shows an example of the fittings below and above the order–disorder phase transition and the parameters obtained are presented in Table 1. Here, as a start, the averaged area per molecule was left as a free parameter and the values obtained were nearly the same for all concentrations and temperatures, and amount to (82±2) Å^2. So, we considered this value as constant for refinement of fittings. The sample with smaller mole fraction of Gemini, x=0.085, showed a constant value of 29 molecules of water bound per polar head, whereas for samples with higher concentration of Gemini the number of bound water molecules

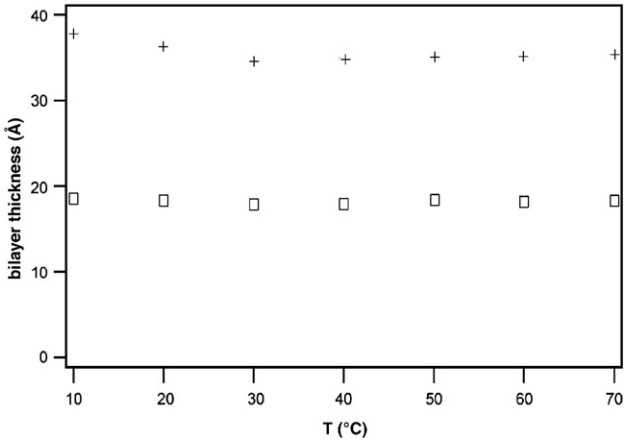

Fig. 5. Variation of the bilayer thicknesses, t_2 (crosses) and t_1 (squares), with temperature, for the system 20 wt.% Gemini in water. Error bars are not shown for being smaller than symbols.

decreases at the non-order/order transition, from (24±2) to (9±2), recovering its initial values after the completion of the ordering process. The variation of t_2 with temperature for all the concentrations studied is shown in Fig. 8a. It also decreases at the order–disorder transition. A constant value of (11.5±0.5) Å was obtained for t_1 for all the samples. The electron densities, ρ_{pol} and ρ_{par}, are also constant, except at the transition temperature, when the L_α phase is formed, at which ρ_{pol} reached a value of 0.400 electrons/Å^3. The value of t_1 indicates that the hydrophobic chains are also interdigitated for mixed samples, as the expected value for t_1 would be 17.5 Å for pure tilted DPPC [35] and 18.4 Å for pure gemini (see above). Considering the averaged area per headgroup, 82 Å^2, we see that it is larger than the area per headgroup of pure DPPC (45.9 Å^2) [35] and of pure gemini (58.8 Å^2, see above). The value obtained is reasonable if we consider that each headgroup occupies the same interfacial area as 4 chains, which can only be possible if the chains are interdigitated. The large cross-section of sugar headgroups, imposing a large lateral pressure, is probably the molecular origin of this generalized tendency for interdigitation of the hydrophobic chains encountered in most of the samples studied.

The more relaxed space between the head-groups is also seen by the larger number of water molecules in the polar region (24 molecules). This value is much larger than that obtained for pure Gemini (7.3) or expected for pure DPPC (10.6) [35]. The total thickness of the half bilayer (27 Å) is slightly larger than the value expected for pure DPPC (24.9 Å) [35]. This gives a thickness of 14.5 Å for the polar shell, which is expected, as the headgroup of Gemini surfactant is much bigger than the DPPC headgroup. Besides, by considering the values obtained for the *d*-spacing of the small part of ordered bilayers at lower temperatures (86.2 Å) one sees that the interbilayer water in the Gemini/DPPC mixtures is approximately 34 Å thick, as the total bilayer thickness has an average value of 52 Å. The swelling relation $d=2t_2/\Phi$, where Φ is the hydrated volume fraction, indicates that only 60% of the volume is occupied by the bilayer at low temperatures. On the other hand, in the L_α phase with the obtained *d*-spacing of 63.1 Å, approximately 80% of the space is occupied by the bilayers, with a water layer of 11 Å. These results evidence a significant dehydration of the sugar heads and of the interbilayer region upon heating. This is consistent with known properties of all single-chain surfactants, such as alkyl polyglucosides [18,36]. With some alkylpolyglucosides, the loss of hydration is large enough to provoke phase separation (cloud point). This is not the case for the catanionic systems, which always remain hydrophilic enough to inhibit phase separation due to loss of solubility in water.

The formation of flat bilayers at high temperatures was observed by Cantù et al. [18], for ganglioside GM3 in water, via loss of water bound to the sugar headgroups, which also caused a decrease in the bilayer thickness. However, in their system the bilayers are not well correlated and only a broad interaction peak is observed. The Gemini/DPPC system exhibits the same number of water molecules bound per surfactant molecule in the polar region (9) and a minimum in the thickness of the hydrophilic shell (9 Å, compared with 14.5 Å at low temperatures), at 50 °C. In our

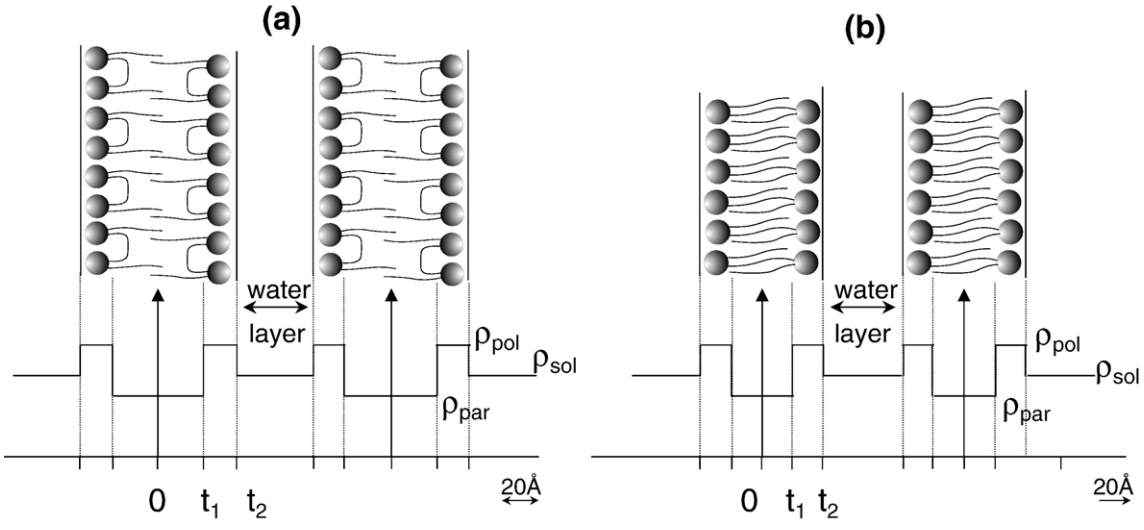

Fig. 6. Models of bilayer used, for Gemini in water with (a) the back-folded spacer and with (b) the extended spacer. ρ_{pol} is the electron density of the polar region, ρ_{par} the electron density of the paraffinic region, ρ_{sol} the electron density of the solvent, t_1 half the thickness of the hydrocarbon region and t_2 half the total thickness of the bilayer.

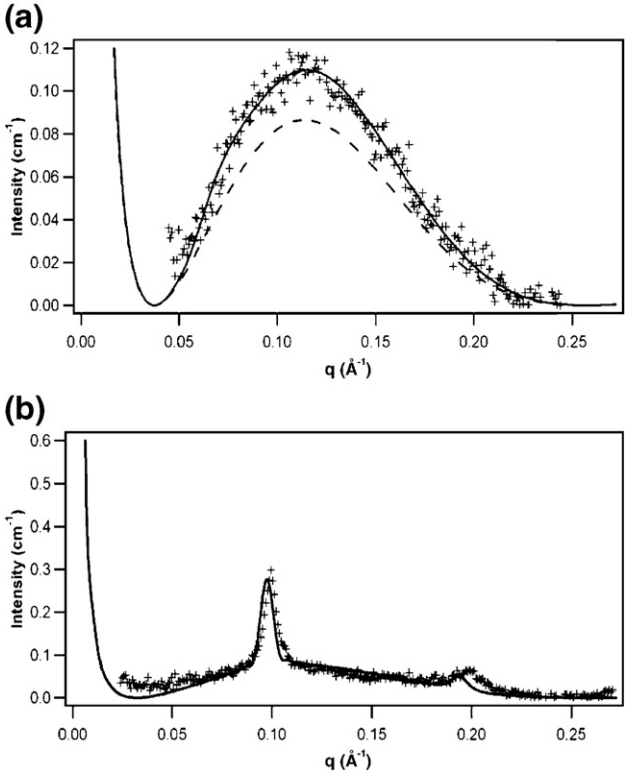

Fig. 7. SAXS curves of the system Gemini/DPPC/water, for $x=0.229$. Crosses: experimental curve; Solid line: modelled curve for the total intensity using Eq. (7); (a) 20 °C; Dashed line: form factor (Eq. (1)); (b) 60 °C.

case, after the rearrangement of the molecules and the formation of the infinite bilayers, above 50 °C, the thickness of the bilayer and the number of hydration water molecules was recovered, whereas the highest temperature studied by Cantù et al. [18] was 50 °C. Notice, however, that in our system the water layer is thinner when the system is ordered at higher temperatures.

Another example of a system that orders at high temperature due to dehydration is the block-copolymer Pluronics (tm) in water. Zhang and Khan [37] and Alexandridis et al. [38] detected dehydration of the hydrophilic parts of the Pluronic L64 (ethylene oxide (EO)-propylene oxide (PO)-ethylene oxide (EO) triblock copolymer ($EO_{13}PO_{30}EO_{13}$)) in water in the lamellar phase with increasing temperature. At low temperature, the well-hydrated headgroups, EO, have a repulsive interaction [39,40]. As the temperature increases, the interaction between the headgroups becomes less repulsive and the distance between the headgroups decreases, changing the order parameter at the same time as dehydration occurs. There are many other studies on pluronic (EO–PO–EO) copolymers which associate loss of hydration by the hydrophilic groups at high temperature with ordering of the system, like stability of highly ordered symmetries [41] or formation of bigger aggregates [42,43]. It must be clarified that in the case of Zhang and Khan [37] and Alexandridis et al. [38] the order parameter refers to the local molecular order, whereas in the present work there is an overall order of the aggregates. Nevertheless, in both cases dehydration is related to the ordering process. In our case, when a great part of the water between the aggregates is lost they tend to grow forming long flat bilayers.

The increase in the number of ordered bilayers N (from 1.5 to 50) and the decrease in the disorder parameter Δ (from 6 to 1) with increasing temperature were evident, although the numbers are interdependent. Even so, the general trend is obvious, as for all concentrations an increase of more than 100% in the number of ordered stacked bilayers was observed, accompanied by a considerable decrease of Δ, the disorder of the bilayers. For all mole fractions studied, we see a decrease in the number of lamellae in the correlated stacks. This demonstrates that infinite bilayers are fragmented. Fragmentation can only occur in the form of discs by continuity of curvature [44].

The suggested model, that at low temperatures the system is formed by two different domains, one consisted of ordered stacked bilayers with frozen chains and the other made of extremely diluted non-correlated flat objects, is confirmed by freeze fracture electron microscopy for 20 wt.% Gemini concentration in water. Fig. 9 shows a well-ordered set of multilayers (multilamellar vesicles) of pure DPPC in the gel phase at 20 °C as well as in the L_α phase at 60 °C. For $x=0.085$, the tendency to form multilamellar vesicles is less pronounced, but at 20 °C spherical multilamellar arrangements can still be detected by means of electron microscopy. For $x=0.334$, a further loss of ordering on the supramolecular level can be observed, and more open curved structures were detected at 20 °C. By heating up the system to 60 °C the lamellae show a more longitudinal orientation and for $x=0.085$ extended rods were predominantly formed. At significantly higher Gemini

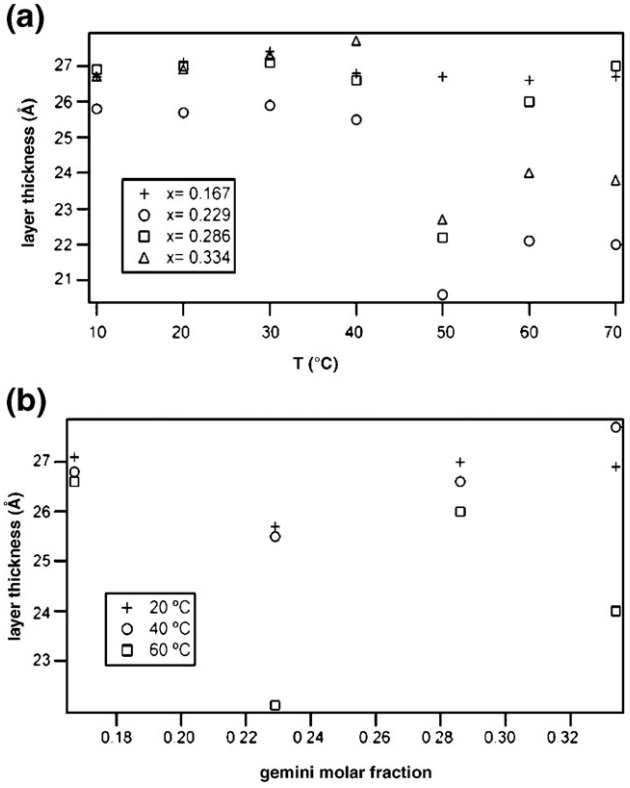

Fig. 8. Variation of the total thickness of the bilayers, t_2, for the system Gemini/DPPC/water. (a) Variation of thickness with temperature, for different Gemini molar fractions. (b) Variation of thickness with Gemini molar fraction, for different temperatures.

concentration (x=0.334) the system becomes more homogeneous, but a longitudinal orientation still exists.

Based on these results, one can conclude that at low temperature the Gemini disturbs the long-range order of the DPPC lamellae. The non-homogeneous distribution of the Gemini molecules, resulting in shorter bilayer segments (see Fig. 10), interferes in the formation of multilamellar vesicles. However, the shorter segments with end-standing Gemini surfactant molecules can still rearrange to spherical multilamellar aggregates, but the supramolecular ordering is significantly lower.

When the temperature increased to 60 °C, the more homogeneous distribution of Gemini in the bilayer leads to larger segments, which tend to form longitudinal ordered structures. In this case, the formation of spherical structures is inhibited.

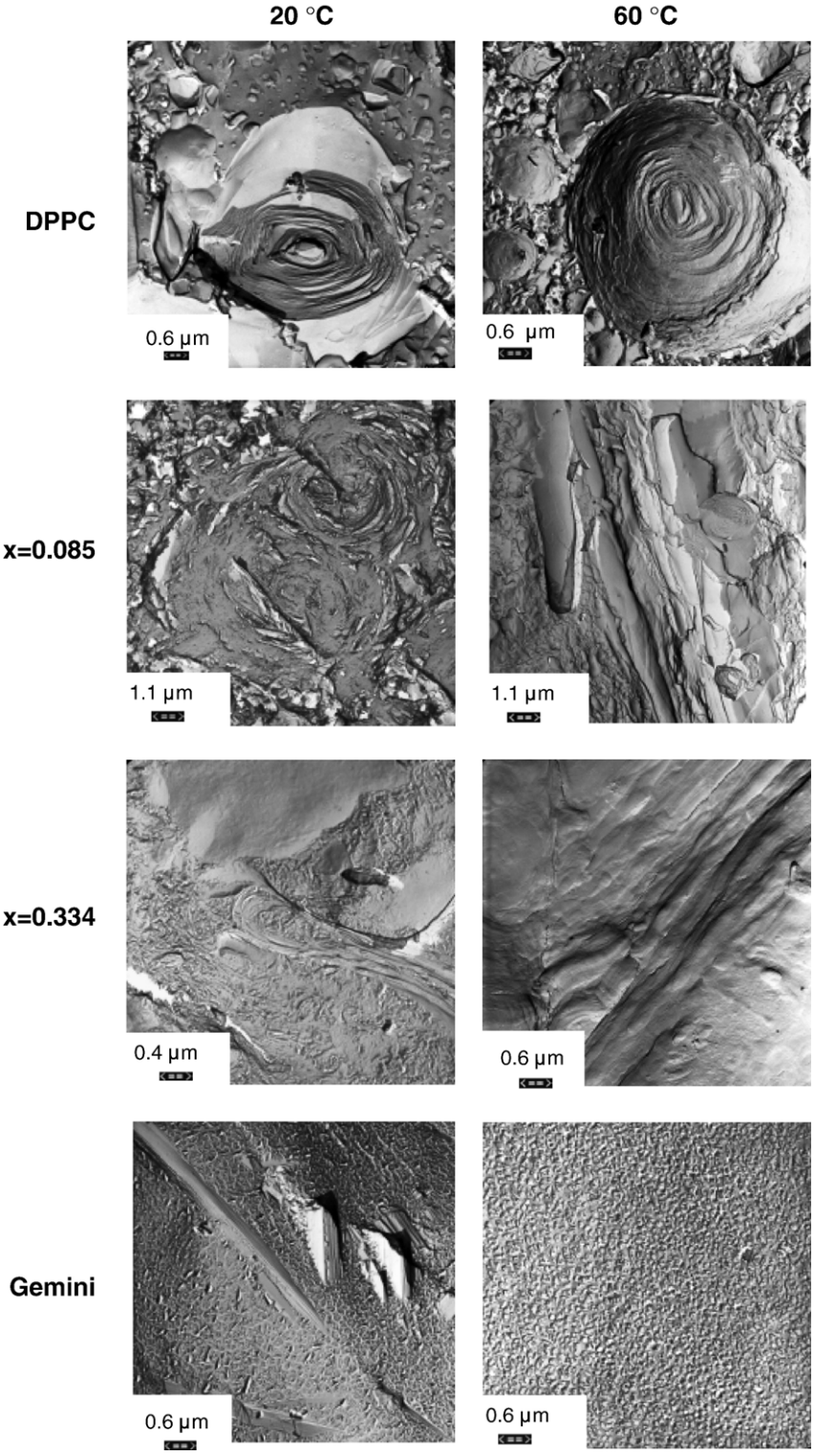

Fig. 9. Micrographs of Gemini/water, DPPC/water and Gemini/DPPC/water at 20 °C and 60 °C, for concentrations of 20 wt.%.

Another striking point is the dependence of t_2 on the Gemini molar fraction. Fig. 8b shows the variation of this parameter for three different temperatures representing the three different trends obtained for the whole set of results, below (20 °C), close (40 °C) and above (60 °C) the melting temperature of the chains. At all temperatures, the values of t_2 are nearly constant, as their variation is inside an error bar of ± 0.5 Å (shown only for one temperature). Thus, we do not have an ideal mixing of both components, as t_2 does not present a linear variation with the Gemini molar fraction.

In-plane miscibility of Gemini with phospholipids is excellent in the molten state, but bellow the chain melting, it decreases and the large dehydrated sugar headgroups form the edges of discs. Infinite bilayers (at high temperature) change to discs by going to lower temperature. This unusual behaviour has already been observed by J. Katsaras and co-workers for mixtures of charged phospholipids [45]. They observed infinite bilayers in mixtures of long- and short-chain lipids at high temperatures, which break down as the temperature decreases, forming a bicellar morphology in which the short-chain lipid concentrates at the edges of the disks, whose flat part is made of the long-chain lipid. In the system studied by Nieh and co-workers even the infinite lamellas have regions with defects, as the short-chain lipid molecules either concentrate at the edges of the bilayers or create "pores" (defects) in the large aggregates. In our system it is also possible that the edges of the disks are mainly formed by Gemini, which, for having two headgroups, will occupy a larger area, whereas the DPPC will be located in the body of the aggregates.

A reversible phase transition (bilayer-micelle) upon temperature decrease has also been observed by Beyer and coworkers [46,47] in mixtures of phospholipids with a non-ionic surfactant, in which the two components are segregated in the micelles with the hydrocarbon chains in the gel state. When the temperature increases and the hydrocarbon chains are molten, both components form bilayers. In this case, however, the bilayers seem not to be ordered, as the SAXS curves present a broad peak even at high temperatures.

A similar order to disorder transition upon cooling has also been observed by Benvegnu et al. [48]. Lecollinet et al. [49] found a transition from an optically isotropic to an ordered phase in

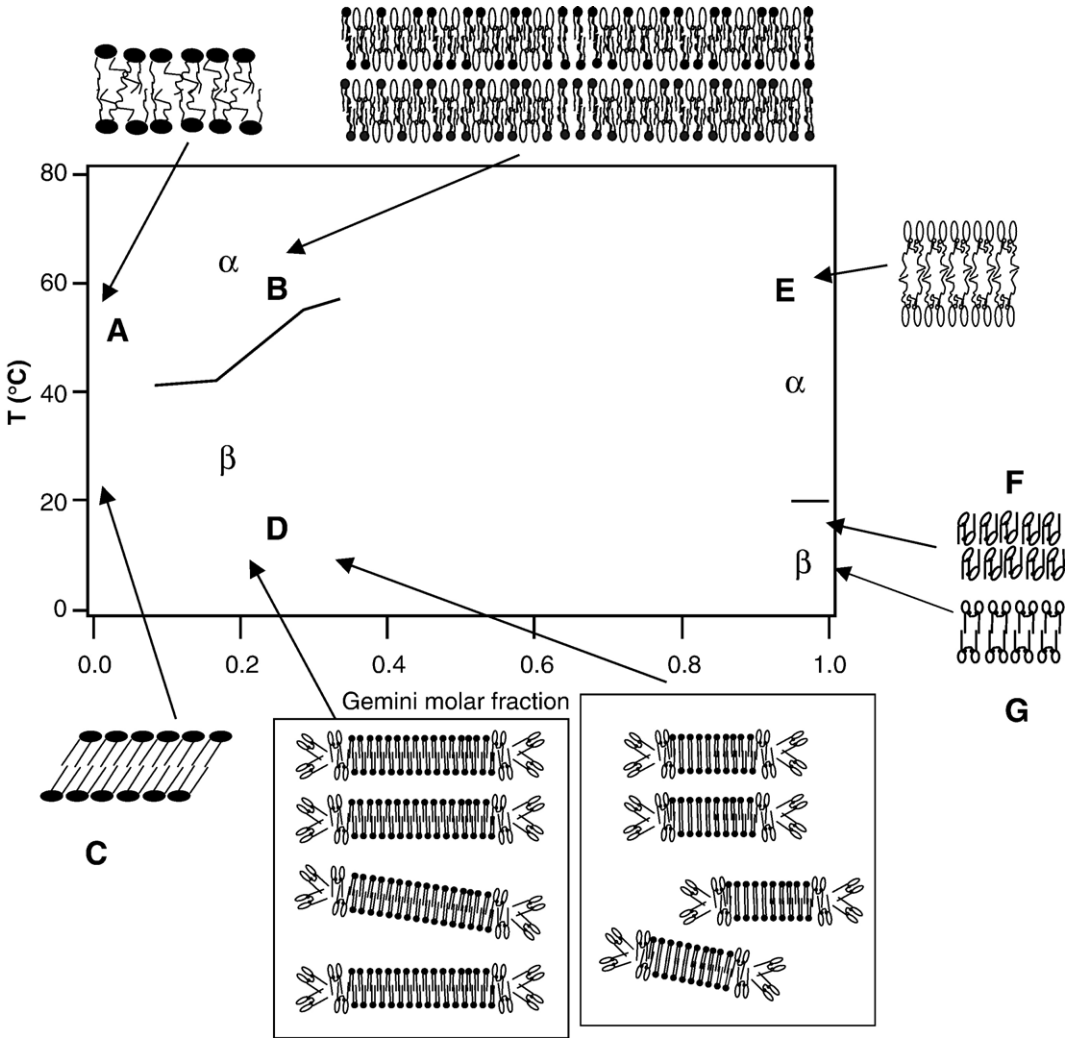

Fig. 10. Proposed phase diagram for the system Gemini/DPPC/water. (A) L_α phase of DPPC; (B) L_α phase of Gemini/DPPC; (C) $L_{\beta'}$ phase of DPPC/water; (D) Non-correlated bilayers of Gemini/DPPC, with crystalline interdigitated chains; (E) Non-correlated Gemini bilayers, with non-interdigitated molten chains; (F) Stacked Gemini bilayers with interdigitated crystalline chains; (G) Stacked non-correlated Gemini bilayers with crystalline non-interdigitated chains.

lipids containing sugar head-groups. The phases involved in this transition were isotropic cubic at low temperatures and a hexagonal phase at higher temperatures.

When small amounts of Gemini are added to the DPPC (notice that in all studied samples the Gemini concentration is smaller than the DPPC), the Gemini has the tendency to be located at the edges of the bilayers, due to the large area requirement mismatch between the compounds: due the presence of two headgroups, separated by the spacer, the cross-sectional area of the Gemini molecules in the configuration of Fig. 6a will be much higher than the cross sectional area of the DPPC molecules. According to the packing parameter [50] the higher area gives the Gemini the tendency to form spherical structures that will be located at the edges of the bilayers.

The small part of Gemini molecules found in the spanning configuration (Fig. 6b) will be placed well inside the apolar region of the bilayers. As just a small percentage of Gemini molecules are in this configuration, as seen from the case of pure Gemini in water, these few molecules of Gemini located inside the hydrophobic region of the bilayers will not be able to affect the overall X-ray scattered intensity, so that the total intensity will correspond to the bilayers formed by a DPPC body with Gemini at the corners. In the pure Gemini system, the pronounced change into the configuration of Fig. 6b might be the reason for the slow kinetics of the gel phase formation. In this case, for being so well ordered, the intensity of this phase will be dominated by the Bragg reflection and the broad peak will correspond to the form factor of the tail-to-tail configuration.

The DPPC main-transition temperature is not affected by the added Gemini. However, the sharp DSC peak with the maximum at 41.8 °C, indicating the melting of the DPPC hydrocarbon chains, becomes significantly smaller and broader [51] after the addition of Gemini, and a peak splitting (40.4 °C and 42.0 °C) is observed. A main-transition enthalpy of 7.9 J/g (7.28 kcal/mole) was obtained for pure DPPC, whereas 0.46 J/g (0.33 kcal/mole) was measured for the sample with a Gemini molar fraction of 0.229. As the enthalpy for the mixed system is so much lower than for pure DPPC, we conclude that a part of the hydrocarbon chains is already molten before the overall melting point observed in the DSC experiments, and possibly some of them could be already molten even before 30 °C (melting temperature of Gemini chains), as we conclude from the WAXS curves of Gemini at 20 °C (Fig. 3b) in which the peak is not as sharp as observed for DPPC [52].

In conclusion, there are three different aspects of the Gemini catanionic surfactants in bilayers. Firstly, when purely mixed with water at high concentration (20 wt.%), it forms small disks in the whole temperature range studied (10 to 70 °C), being abundant surrounded by water. The crystalline/non-crystalline state of the hydrocarbon chains has no influence on these aggregates, and the hydrocarbon chains are mostly non-interdigitated. Secondly, at temperatures lower than 30 °C it forms lamellae which are very poorly hydrated and arranged with the extended spacer (binding two headgroups at opposing ends, as in Fig. 6b). These last results comfort our hypothesis that, at low concentration (2 wt.%), the masked hydrophobicity of the Gemini is responsible for its high anti-HIV activity as well as its low toxicity [8].

Finally, when mixed in the frozen (gel) state in DPPC bilayers, segregation occurs promoting interdigitation of the chains, and the general organisation of the bilayers is a dispersion of small non-correlated disks with catanionics. The rearrangement into microdomains of Gem16-12 in DPPC bilayers confirms the difficulty of this compound in incorporating in phospholipid membranes, which is in agreement with its low toxicity. Upon heating, the interbilayer water is expelled and infinite ordered bilayers in the highly repulsive L_α phase are present. The peaks are very sharp, due to the electric charge, as shown by G. Brotons et al. [53]. The bilayers at high temperature have nearly the same thickness as the disks at low temperature. According to our discussion, we propose the phase diagram presented in Fig. 10. In all mentioned cases, the ordering process was accompanied by dehydration.

Acknowledgements

The authors thank Prof. Th. Zemb for his valuable contribution to the discussion of this work. We thank Dr. S. S. Funari and M. Dommach for the assistance at the beam-line A2 at HASYLAB (DESY, Hamburg, Germany), O. Taché for the control experiments and absolute scaling experiments performed in Saclay and Dr. B. Tiersch for the freeze fracture EM micrographs. This work has been supported by the French-German CEA/CNRS/DFG/MPG network "Thin films of complex fluids: from two to three dimensions".

References

[1] J. Fantini, N. Yahi, Galactosyl ceramide, a new receptor for the human-immunodeficiency virus (HIV), MS Med. Sci. 9 (1993) 891–900 (and references therein).

[2] R. Villard, D. Hammache, G. Delapierre, F. Fotiadu, G. Buono, J. Fantini, Asymmetric synthesis of water-soluble analogues of galactosylceramide, a HIV-1 receptor: new tools to study virus glycolipid interactions, Chem. BioChem. 3 (2002) 517–525;
B. Faroux-Corlay, J. Greiner, R. Terreux, D. Cabrol-Bass, A.M. Aubertin, P. Vierling, J. Fantini, Amphiphilic anionic analogues of galactosylceramide: synthesis, anti-HIV-1 activity, and gp120 binding, J. Med. Chem. 44 (2001) 2188–2203;
I. Rico-Lattes, M.F. Gouzy, C. Andre-Barres, B. Guidetti, A. Lattes, Synthetic bolaamphiphilic analogues of galactosylceramide (GalCer) potentially binding to the v3 domain of HIV-1 gp120: key-role of their hydrophobicity, N.J. Chem. 22 (1998) 451–457;
J. Fantini, D. Hammache, O. Delezay, N. Yahi, I. Rico-Lattes, A. Lattes, Synthetic soluble analogs of galactosylceramide (GalCer) bind to V3 domain of HIV-1 gp120 and inhibit HIV-1-induced fusion and entry, J. Biol. Chem. 272 (1997) 7245–7252;
C.R. Bertozzi, D.G. Cook, W.R. Kobertz, F. Gonzalez-Scarano, M.D. Bednarski, Carbon-linked galactosphingolipid analogs bind specifically to HIV-1 gp120, J. Am. Chem. Soc. 114 (1992) 10639–10641.

[3] M. Tateno, F. Gonzalez-Scarano, J.A. Levy, Human immunodeficiency virus can infect CD4-negative human fibroblastoid cells, Proc. Natl. Acad. Sci. U. S. A. 86 (1989) 4287–4290;
J.M. Harouse, C. Kunsch, H.T. Hartle, M.A. Laughlin, J.A. Hoxie, B. Wigdahl, F. Gonzalez-Scarano, CD4-independent infection of human neural cells by human immunodeficiency virus type-1, J. Virol. 63 (1989) 2527–2533.

[4] J.M. Harouse, S. Bhat, S.L. Spitalnik, M. Laughlin, K. Stefano, D.H. Silderberg, F. Gonzalez-Scarano, Inhibition of entry of HIV-1 in neural cell lines by antibodies against galactosyl ceramide, Science 253 (1991) 320–323;

N. Yahi, S. Baghdiguian, M. Moreau, J. Fantini, Galactosyl ceramide (or a closely related molecule) is the receptor for human-immunodeficiency virus type-1 on human colon epithelial ht29 cells, J. Virol. 66 (1992) 4848–4854.
[5] E.W. Kaler, A. Kamalakara Murthy, B.E. Rodriguez, J.A.N. Zasadzinski, Spontaneous vesicle formation in aqueous mixtures of single-tailed surfactant, Science 245 (1989) 1371–1374;
F.E. Menger, W.H. Binder, J.S. Keiper, Cationic surfactants with counterions of glucuronade glycosides, Langmuir 13 (1997) 3247–3250;
C. Tondre, C. Caillet, Properties of the amphiphilic films in mixed cationic/anionic vesicles: a comprehensive view from a literature analysis, Adv. Colloid Interface Sci. 93 (2001) 115–134.
[6] M. Blanzat, E. Perez, I. Rico-Lattes, D. Promé, J.C. Promé, A. Lattes, New catanionic glycolipids. 1. Synthesis, characterization, and biological activity of double-chain and gemini catanionic analogues of galactosylceramide (gal$\beta_1$cer), Langmuir 15 (1999) 6163–6169.
[7] M. Blanzat, E. Perez, I. Rico-Lattes, A. Lattes, Synthesis and anti-HIV activity of catanionic analogs of galactosylceramide, New J. Chem. 23 (1999) 1063–1065.
[8] M. Blanzat, E. Perez, I. Rico-Lattes, A. Lattes, A. Gulik, Correlation between structure, aggregation behaviour and cellular toxicity of anti-HIV catanionic analogues of galactosylceramide, Chem. Commun. 2 (2003) 244–245;
M. Blanzat, Premiers analogues catanioniques du galactosylcéramide, Synthèse ciblée et évaluation de leurs propriétes anti-HIV, Université Paul-Sabatier, toulouse (France), 2000 (28 September).
[9] A. Brun, G. Brezesinski, H. Möhwald, M. Blanzat, E. Perez, I. Rico-Lattes, Interaction between phospholipids and new Gemini catanionic surfactants having anti-HIV activity, Colloids Surf., A 228 (2003) 3–16.
[10] M. Dubois, T. Gulik-Krzywicki, B. Deme, Th. Zemb, Rigid organic nanodisks of controlled size: a catanionic formulation, C. R. Acad. Sci., Ser. II, Fasicule C-Chim. 1 (1998) 567–575.
[11] M. Dubois, Th. Zemb, Swelling limits for bilayer microstructures: the implosion of lamellar structure versus disordered lamellae, Curr. Opin. Colloid Interface Sci. 5 (2000) 27–37.
[12] F. Ricoul, M. Dubois, T. Zemb, D. Plusquellec, Micelles-smetic phase coexistence: origin of the maximum swelling of a mixed lamellar phase, Eur. Phys. J., B 4 (1998) 333–340.
[13] F. Ricoul, M. Dubois, L. Belloni, Th. Zemb, Ch. André-Barrès, I. Rico-Lattes, Phase equilibria and equation of state of a mixed cationic surfactant–glycolipid lamellar system, Langmuir 14 (1998) 2645–2655.
[14] J. Zimmerberg, L.V. Chermordik, Membrane fusion, Adv. Drug Delivery Rev. 38 (3) (1999) 197–205.
[15] R. Garelli-Calvet, P. Latge, I. Rico-Lattes, A new surfactant series, the n-alkylamino-1-deoxylactitols—Application for extraction of op opiate receptors from frog brain, Biochim. Biophys. Acta 1109 (1992) 55–58.
[16] A. Gabriel, F. Dauvergne, The localization method used at EMBL, Nucl. Instrum. Methods Phys. Res. 201 (1982) 223–224.
[17] T. Zemb, O. Tache, F. Né, O. Spalla, A high sensitivity pinhole camera for soft condensed matter, J. Appl. Crystallogr. 36 (2003) 800–805.
[18] L. Cant'u, M. Corti, E. DelFavero, M. Dubois, T.N. Zemb, Combined small-angle X-ray and neutron scattering experiments for thickness characterization of ganglioside bilayers, J. Phys. Chem., B 102 (1998) 5737–5743.
[19] B. Cabane, T. Zemb, Water in the hydrocarbon core of micelles, Nature 314 (1985) 385.
[20] L. Cantù, M. Corti, E. Del Favero, M. Dubois, T. Zemb, Consistency of microstructural modeling of micelles: letter concerning "thermotropic behaviour and stability of monosialoganglioside micelles in aqueous solution", Biophys. J. 74 (3) (1998) 1600–1603.
[21] P.J. Alonso, J.A. Puértulas, P. Davidson, B. Martinez, J.I. Martinez, L. Oriol, J.L. Serrano, X-ray and magnetic characterization of a nematic polyester based on a metallomesogenic copper (II) moiety, Macromolecules 26 (1993) 4304–4309.
[22] M.P.B. van Bruggen, J.K.G. Dhont, H.N.W. Lekkerkerker, Morphology and kinetics of the isotropic–nematic phase transition in dispersions of hard rods, Macromolecules 32 (1999) 2256–2264.
[23] A.E. Blaurock, Evidence of bilayer structure and of membrane interactions from X-ray diffraction analysis, Biochim. Biophys. Acta 650 (1982) 167–207.
[24] T. Zemb, M. Dubois, B. Deme, T. Gulik-Krzywicki, Self-assembly of flat nanodiscs in salt-free catanionic surfactant solutions, Science 283 (1999) 816–819.
[25] Y. Lyatskaya, Y. Liu, S. Tristan-Nagle, J. Katsaras, J.F. Nagle, Method for obtaining structure and interactions from oriented lipid bilayers, Phys. Rev. E 63 (2000) 11907/1–11907/9.
[26] R. Zhang, R.M. Suter, J.F. Nagle, Theory of the structure factor of lipid bilayers, Phys. Rev. E 50 (1994) 5047–5060.
[27] G. Pabst, M. Rappolt, H. Amenitsch, P. Laggner, Structural information from multilamellar liposomes at full hydration: full q-range fitting with high quality X-ray data, Phys. Rev. E 62 (2000) 4000–4009.
[28] R. Hosemann, S.N. Bagchi, Direct Analysis of Diffraction by Matter, North-Holland Publishing Co., Amsterdam, 1962.
[29] A. Guinier, X-ray Diffraction in Crystals, Imperfect Crystals and Amorphous Bodies, W.H. Freeman, S. Francisco, 1963.
[30] J. Koetz, B. Tiersch, I. Bogen, Polyelectrolyte-induced vesicle formation in lamellar liquid crystalline model systems, Colloid Polym. Sci. 278 (2000) 164–168.
[31] M. Dubois, T. Zemb, Phase behavior and scattering of double-chain surfactants in diluted aqueous solutions, Langmuir 7 (1991) 1352–1360.
[32] B.L. Bales, A.M. Houwe, A.R. Pitt, J.A. Roe, P.C. Griffiths, A spin-probe study of the modification of the hydration of SDS micelles by insertion of sugar-based nonionic surfactants molecules, J. Phys. Chem., B 104 (2000) 264–270.
[33] C. Dupuy, X. Auvray, C. Petipas, R. Anthore, I. Rico-Lattes, A. Lattes, Influence of structure of polar head on the micellization of lactose-based surfactants. Small-angle X-ray and neutron scattering study, Langmuir 14 (1998) 91–98.
[34] B.L. Bales, R. Ranganathan, P.C. Griffiths, Characterization of mixed micelles of SDS and sugar-based noionic surfactant as a variable reaction medium, J. Phys. Chem., B 105 (2001) 7465–7473.
[35] M.C. Wiener, R.M. Suter, J.F. Nagle, Structure of the fully hydrated gel phase of dipalmitoylphosphatidylcholine, Biophys. J. 55 (1989) 315–325.
[36] F. Nilsson, O. Söderman, I. Johansson, Physical chemical properties of the n-octyl β-D-glucoside/water system. A phase diagram, self-diffusion NMR, and SAXS study, Langmuir 12 (1996) 902–908.
[37] K.W. Zhang, A. Khan, Phase behavior of poly(ethylene oxide)-poly (propylene oxide)-poly(ethylene oxide) triblock copolymers in water, Macromolecules 28 (1995) 3807–3812.
[38] P. Alexandridis, D.L. Zhou, A. Khan, Lyotropic liquid-crystallinity in amphiphilic block copolymers: temperature effects on phase behavior and structure for poly(ethylene oxide)-b-poly(propylene oxide)-b-poly(ethylene oxide) copolymers of different composition, Langmuir 12 (1996) 2690–2700.
[39] R. Kjellander, E. Florin, Water structure and changes in thermal stability of the system poly (ethylene-oxide)-water, J. Chem. Soc., Faraday Trans. 1 (77) (1981) 2053.
[40] R. Kjellander, Phase separation of non-ionic surfactant solutions—A treatment of the micellar interaction and form, J. Chem. Soc., Faraday Trans. 2 (78) (1982) 2025–2042.
[41] M. Svensson, P. Alexandridis, P. Linse, Phase behavior and microstructure in binary block copolymer/selective solvent systems: experiment and theory, Macromolecules 32 (1999) 637–645.
[42] B. Svensson, U. Olsson, P. Alexandridis, K. Mortensen, A SANS investigation of reverse (water-in-oil) micelles of amphiphilic block copolymers, Macromolecules 32 (1999) 6725–6733.
[43] M.C. Gerstenberg, J.S. Pedersen, J. Majewski, G.S. Smith, Surface induced ordering of triblock copolymer micelles at solid–liquid interface. 1. Experimental results, Langmuir 18 (2002) 4933–4943.
[44] S. Hyde, in: S. Andersson, K. Larsson, Z. Blum, T. Landh, S. Lidin, B.W. Ninham (Eds.), The Language of Shape: The Role of Curvature in Condensed Matter: Physics, Chemistry and Biology, Elsevier Science B.V., 1997.
[45] M.-P. Nieh, C.J. Glinka, S. Krueger, R.S. Prosser, J. Katsaras, SANS study of the structural phases of magnetically alignable lanthanide-doped phospholipid mixtures, Langmuir 17 (2001) 2629–2638.
[46] D. Otten, L. Lobbecke, K. Beyer, Stages of the bilayer-micelles transition in the system phosphatidylcholine-C(12) E (8) as studied by deuterium-NMR

and phosphorus-NMR, light-scattering and calorimetry, Biophys. J. 68 (1995) 584–597.
[47] S.S. Funari, B. Nuscher, G. Rapp, K. Beyer, Detergent–phospholipid mixed micelles with a crystalline phospholipid core, Proc. Natl. Acad. Sci. U. S. A. 98 (2001) 8938–8943.
[48] T. Benvegnu, G. Lecollinet, J. Guilbot, M. Roussel, M. Brard, D. Plusquellec, Novel bolaamphiphiles with saccharidic polar headgroups: synthesis and supramolecular self-assemblies, Polym. Int. 51 (2002) 1–8.
[49] G. Lecollinet, A. Gulik, G. Mackenzie, J.W. Goodby, T. Benvegnu, D. Plusquellec, Supramolecular self-assembling properties of membrane-spanning archaeal tetraether glycolipid analogues, Chem.-Eur. J. 8 (2002) 585–593.
[50] J.N. Israelachvili, D.J. Mitchell, B.W. Ninham, Theory of self-assembly of hydrocarbon amphiphiles into micelles and bilayers, J. Chem. Soc., Faraday Trans. 72 (1976) 1525–1568.
[51] M.T. Lamy-Freund, K.A. Riske, The peculiar thermo-structural behavior of the anionic lipid DMPG, Chem. Phys. Lipids 122 (2003) 19–32.
[52] T.H. Huang, C.W.B. Lee, S.K. Dasgupta, A. Blume, R.G. Griffin, A C-13 and H-2 nuclear magnetic resonance study of phosphatidylcholine cholesterol interactions—Characterization of liquid–gel phases, Biochemistry 32 (1993) 13277–13287.
[53] G. Brotons, T. Salditt, M. Dubois, Th. Zemb, Highly oriented, charged multilamellar membranes osmostically stressed by a polyelectrolyte of the same sign, Langmuir 19 (2003) 8235–8244.